SAND96-1448C
CONF-970135--16

HOW GEOMETRIC DETAILS CAN AFFECT THE STRENGTH OF ADHESIVE LAP JOINTS

K. E. Metzinger and T. R. Guess

Sandia National Laboratories
Albuquerque, New Mexico

ABSTRACT

The durability of adhesively bonded joints - when utilized as blade attachments - has a significant impact on the performance of wind turbines. Accordingly, there is interest in determining how geometric details affect the strength of these joints. Finite element analyses were performed to aid in the selection of three composite-to-metal joint geometries for compressive axial testing. Both monotonic and low-cycle fatigue tests were conducted. Analysis and testing of these joints provide insight into the effects of adding extra adhesive to the end of the bond or tapering the metal adherend. The issue of whether the relative performance of different joints in monotonic tests can be used to predict the relative fatigue strength of these joints is also addressed.

INTRODUCTION

Adhesively bonded lap joints are often used in wind turbines as blade attachments. Because these attachments are critical to the turbine performance, various modifications have been made to these joints in hopes of increasing their service lives. A combination of analyses and testing are employed in this study in an effort to establish whether a few common modifications are worthwhile. Specifically, the effects of adding extra adhesive to the end of the bond or tapering the metal adherend are addressed. Some preliminary finite element analyses were performed to arrive at the three tubular lap joint geometries considered in this study. The baseline design employs an adhesive bond of constant thickness which is truncated at the ends of uniform adherends. The first variation is comprised of uniform adherends with extra adhesive at the end of the metal (steel) adherend. The second variation has a tapered steel adherend with the adhesive truncated at the end of the adherends. A schematic of the joint geometries considered in this study is shown in Figure 1. These analyses predicted that significant differences in the adhesive peel stresses and plastic strains would develop in the various joints when they were subjected to the same compressive load. Although no criteria have been established for quantifying when a joint will fail, it was anticipated that differences in the peel stress and/or the plastic strain in the adhesive would correspond to differences in the strengths of the joints.

Compressive testing was employed in this study primarily because the specimens are easier (and less expensive) to manufacture since no accommodations must be made for gripping the ends. It should be noted that the best joint geometry for compressive loads may not be the best geometry for tensile loads. However, the purpose of this study is to establish if minor modifications affect the strength of joints and, if so, how to predict the effect of such changes. After the specimen designs were finalized and the samples were fabricated, monotonic destructive tests of the three joint geometries were conducted. The baseline design joints failed at slightly higher loads than the joints with the tapered adherend design. For both geometries, failure occurred when the adhesive debonded from the steel adherend. However, the

DISCLAIMER

specimens with extra adhesive failed - at significantly higher levels - when the composite delaminated at the end of the test specimens; the joints didn't actually fail. Subsequently, low-cycle (up to 10^5) fatigue tests were conducted. Ultrasonic inspection was used to detect if the adhesive had debonded from the steel adherend. Despite the limited data, the joints with extra adhesive again appear to be superior to both the baseline and tapered adherend geometries. To a lesser extent, the tapered adherend joints appear to perform better in low-cycle fatigue than the baseline joints.

Post-test finite element analyses were then performed (with finer meshes than were used in the pre-test analyses) in an attempt to determine if the peel stresses and/or the plastic strains in the adhesive could be used to 'predict' the test results. For the monotonic tests, the peel stress appears to be a good indicator of the relative strengths for the three geometries considered. For the low-cycle fatigue tests, the plastic strain may also need to be considered. Although no high-cycle fatigue tests were conducted in this study, it is anticipated that the plastic strain in the adhesive will also be important for these conditions. In this study, the results of the monotonic tests weren't always suitable for predicting the relative low-cycle fatigue lives of the joints. Thus, using the results of monotonic tests to predict the relative performance of joints in high-cycle fatigue could be quite misleading.

EXPERIMENTS

1. Procedures

The specimens were compressed between two platens in an electrohydraulic test frame, as shown in Figure 2. The typical specimen was instrumented with three strain gages, spaced equally around the circumference of the composite tube. The lower platen rotates on a spherical seat. Prior to loading at high levels, the samples were lightly loaded and the lower platen was adjusted until the strain gages indicated that the specimen was being subjected to a uniform axial strain. During the monotonic tests, the specimens were loaded incrementally to failure, with brief pauses to record the data. In the cyclic tests, the specimens were alternately subjected to a predetermined number of cycles at 2 to 4 Hz, then ultrasonically inspected to determine if the adhesive had debonded from the steel adherend. A ratio of 10 was used for the maximum to minimum compressive load for all of the cyclic tests.

2. Monotonic Test Results

Figure 3 shows the failure loads for the monotonically-loaded specimens. Several points should be made regarding these results. The joints with the baseline and tapered adherend designs failed when the adhesive debonded from the steel adherend. The joints with the extra adhesive didn't actually fail; the loads reported are the levels at which the composite tubes delaminated (at their ends). On three of the four joints with the tapered adherends, a loud popping noise was heard well before the joint completely failed. The strain gage data from one of these joints is shown in Figure 4 and suggests that the adhesive partially debonded from the steel (leading to nonuniform loading) prior to total joint failure. Clearly, the joints with the extra adhesive are the strongest when monotonically loaded to failure. While the scatter in the baseline joints makes comparisons more difficult, the better baseline joints are clearly stronger than the better joints with tapered adherends.Thus, the baseline joints are judged to be stronger than the joints with the tapered adherends, especially if the initial adhesive debonding in the joints with the tapered adherends is considered a failure.

3. Cyclic Test Results

Figure 5 shows the results of the low-cycle fatigue tests. Each data point represents the number of cycles a joint withstood for a given loading cycle before the adhesive was first determined to have debonded from the steel adherend. Several of the data points represent an upper bound on the number of cycles, primarily because the ultrasonic inspections were too infrequent. Along with the limited number of samples, this makes comparisons of the various geometries more difficult. Still, for the tests with a maximum compressive load of 20000 lb, the extra adhesive joint withstood roughly 100 times more cycles than the other two joints. To a lesser extent, the tapered adherend joints endured more cycles than the baseline joints for both the 15000 and 20000 lb tests. Thus, the following two interpretations of the data are offered. As with the monotonic tests, the joints with the extra adhesive perform the best in low-cycle fatigue tests. Reversing the trend seen in the monotonic tests, the joints with the tapered adherends have longer low-cycle fatigue lives than the baseline joints.

ANALYSES

1. Finite Element Model

Figure 6 shows the axisymmetric finite element mesh used for the baseline composite (outer) on steel (inner) tubular lap joint. The adhesive layer - which is shaded in Figure 6 - is 0.1 inches thick and has eight elements through the thickness. The steel and composite adherends are 0.275 and 0.250 inches thick and extend 3.0 and 2.56 inches beyond the bond on either side, respectively. (The composite also extends slightly beyond the other end of the bond as a result of the manufacturing process). The bond is 3 inches long. The outer surface of the outer adherend has a radius of 1.5 inches. Figure 7 shows portions of the two alternate meshes; the adhesive elements are again shaded. All of the meshes are comprised of four-node bilinear (CAX4) axisymmetric solid elements. ABAQUS [1] was used for the analyses, which incorporate nonlinear geometric effects and allow for plastic deformations in the adhesive. The isotropic material properties used for the adhesive and the steel are listed in Table 1. The adhesive properties represent Hysol EA-9394, a high strength, room-temperature curing paste adhesive. The orthotropic material properties listed in Table 2 represent a plain weave E-glass fabric/epoxy composite. The subscripts r, a, and t in Table 2 refer to the radial, axial, and tangential directions, respectively. The material property values used for the adhesive and the composite were taken from [2] and [3]. Generic values were used for the steel.

2. Results

Figure 8 shows how the computed peel stresses in the adhesive vary along the length of the bonds when the joints are subjected to a compressive axial load of 40000 lb - a representative failure load. The values shown are taken at the steel adherend/adhesive interface (the failure location). Since the deformed shapes of the joints are used to generate these plots, the ends of the steel adherends correspond to bond distances of approximately, but not exactly, 3 inches. Figure 9 shows the plastic strains for the same analyses. Several points should be made about the information contained in Figures 8 and 9. Note that a fine mesh is required to capture the peel stresses at the end of the bond. In addition, the peel stresses and the plastic strains are much higher at the end of the bond where the load is transferred to the more compliant adherend. Thus, debonding would be predicted to initiate at this end - as was observed in the cyclic testing. Also note that the adhesive doesn't yield over a significant portion of the bond length. Thus, the bond is considered to be of sufficient length. That is, a longer bond would be expected to behave similarly, although a much shorter bond might not. It is easy to distinguish the predicted peel stresses in the baseline and the tapered adherend joints from those in the extra adhesive geometry. However, it is uncertain whether the much smaller differences between the computed peel stresses in the baseline and the tapered adherend joints are significant because the results of these analyses are mesh-dependent and the area over which failure initiates is unknown.

If only the peel stresses in the adhesive are considered, the joints with the extra adhesive would be expected to be stronger than the other two geometries since the large peel stresses that develop in these joints are compressive instead of tensile. Indeed, these joints performed the best in both the monotonic and the low-cycle fatigue tests. However, this criterion cannot explain why the baseline joints performed better than the tapered adherend joints in the monotonic tests, while the reverse was true for the low-cycle tests. If the plastic strain levels become a significant factor in the low-cycle fatigue tests, the joints with tapered adherends would be expected to perform better than the baseline joints - as was observed. It is less clear why the baseline joints performed better than those with the tapered adherends in the monotonic tests since the geometries develop comparably high tensile peel stresses. One possibility is that the residual stresses due to the adhesive shrinkage during curing are higher for the joints with the tapered adherends. The actual curing processes of adhesives are quite complex. However, assuming the curing process to be a uniform volumetric contraction should provide qualitative insights into whether the differences in the residual stresses that develop in the various geometries might be significant.

Figure 10 shows how the computed peel stresses in the adhesive vary along the length of the bonds when the adhesives undergo a 0.3% volumetric contraction. This corresponds to the amount of global contraction that the adhesive used in these joints undergoes when cured at room temperature. It should be noted that many adhesives shrink considerably more than this amount when cured. Regardless of the amount of contraction, note that the tapered adherend joints develop higher peel stresses at the end of the bond than the baseline joints. Thus, higher residual peel stresses in the adhesive due to curing could be a factor in the underperformance of the tapered adherend joints relative to the baseline joints in the monotonic tests. Even if this is not the case, the data in Figure 10 suggests that residual stresses due to curing should be considered when evaluating different designs. Furthermore, the adhesive peel stresses which develop due to thermal cycling of the joints while in service should also be considered when evaluating competing designs.

SUMMARY

Various modifications are being made to composite-to-metal adhesive lap joints in an effort to increase their service lives. In this study, the effects of adding extra adhesive to the end of the bond and of tapering the metal adherend are considered. Compressive axial testing of three different joint geometries revealed that specimens with extra adhesive had higher monotonic strengths and longer low-cycle fatigue lives than the other two joint geometries. The apparent reason is that these joints don't develop high tensile peel stresses under compressive loading like the other joints do. To a lesser extent, the baseline joints were stronger than the tapered joints in the monotonic tests, but had shorter lives in the low-cycle fatigue tests. The explanation proposed in this study is that these geometries develop similar adhesive peel

stresses, but significantly different plastic strains. The extent of the adhesive yielding is believed to become a factor in the low-cycle fatigue tests. It is presumed that the plastic strains in the adhesive will also be important for high-cycle fatigue applications. Thus, selecting a design for long service from a variety of choices based on the results of monotonic tests would be imprudent.

ACKNOWLEDGMENTS

E. D. Reedy, Jr. shared his insights into the behavior of adhesive lap joints. M. E. Stavig was instrumental in the testing of the joints. This work was performed at Sandia National Laboratories, which is operated for the U. S. Department of Energy under Contract No. DE-AC04-94AL85000.

REFERENCES

1. ABAQUS/Standard, Version 5.5.
2. T. R. Guess, E. D. Reedy, Jr., and M. E. Stavig, "Mechanical Properties of Hysol EA-9394 Structural Adhesive," SAND95-0229, Sandia National Laboratories, Albuquerque, New Mexico, February 1995.
3. T. R. Guess, E. D. Reedy, Jr., and A. M. Slavin, "Testing Composite-to-Metal Tubular Lap Joints," *Journal of Composites Technology & Research*, Vol. 17, No. 2, April 1995.

Table 1: Isotropic Material Properties

Material	Elastic Modulus (psi)	Poissons Ratio	Yield Strength (psi)	Hardening Modulus (psi)
Adhesive	6×10^5	0.37	4×10^3	3×10^5
Steel	3×10^7	0.30	-	-

Table 2: Orthotropic Material Properties (Composite)

E_r (psi)	E_a (psi)	E_t (psi)	υ_{ra}	υ_{rt}	υ_{at}	G_{ra} (psi)	G_{rt} (psi)	G_{at} (psi)
1.45×10^6	3.26×10^6	4.06×10^6	0.10	0.10	0.17	7.25×10^5	7.25×10^5	7.25×10^5

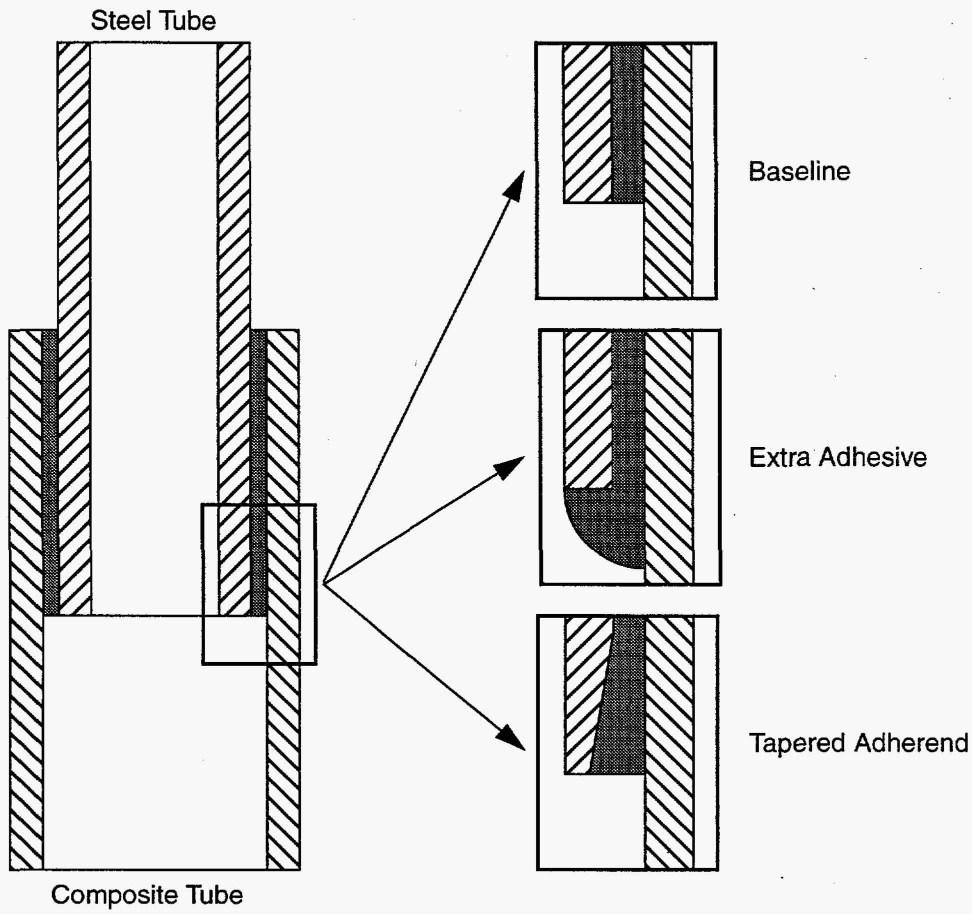

Figure 1. Schematic of Joint Geometries (Cut-Away View)

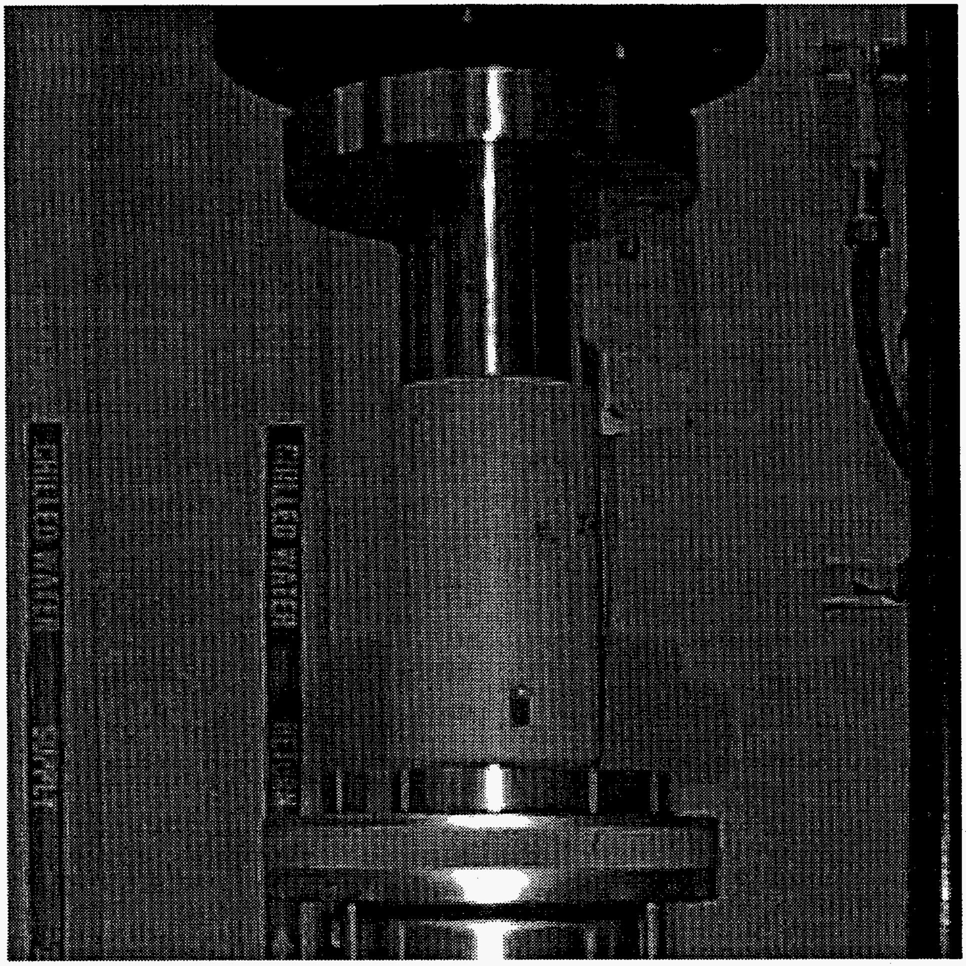

Figure 2. Test Setup

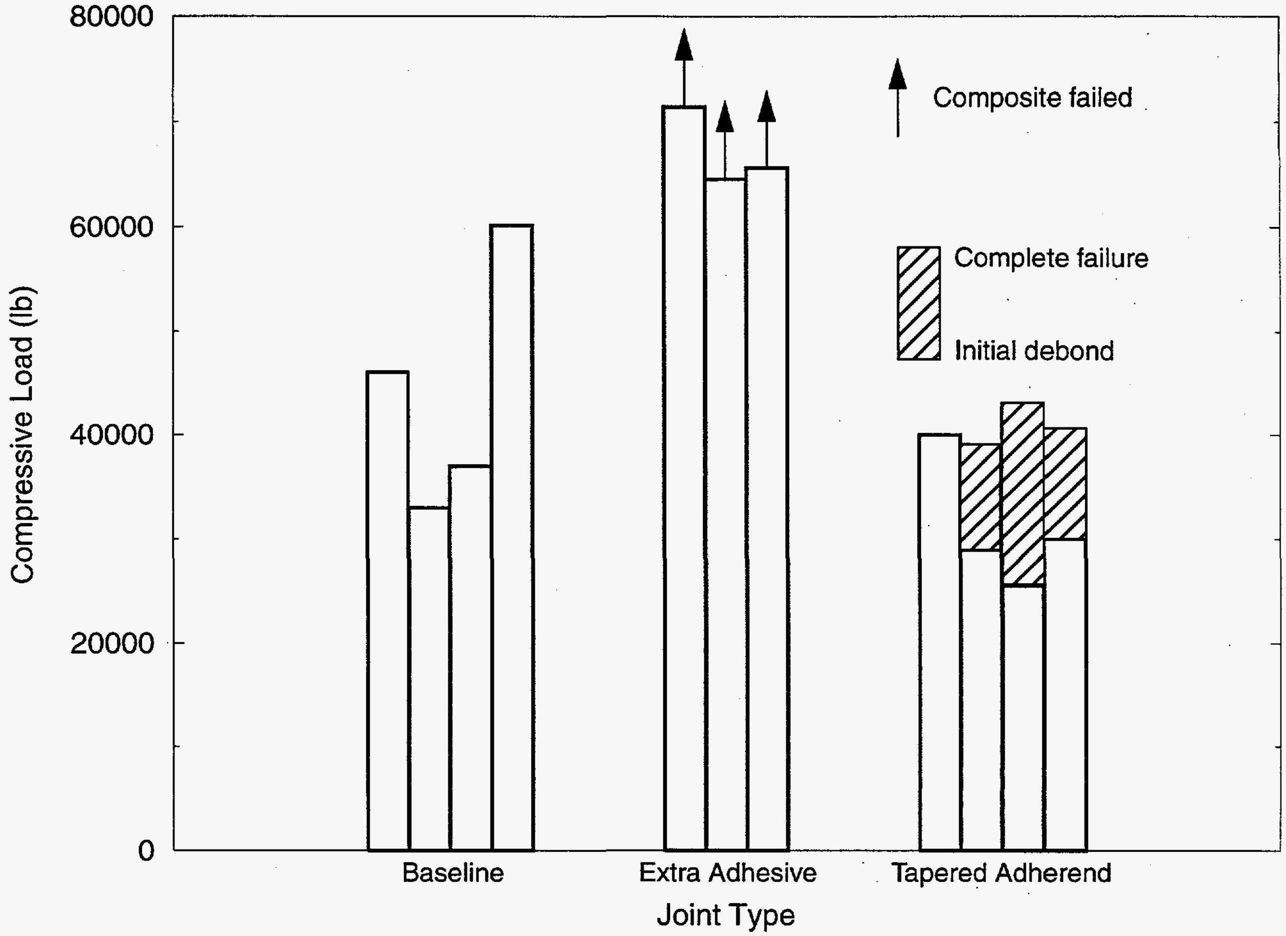

Figure 3. Monotonic Test Results

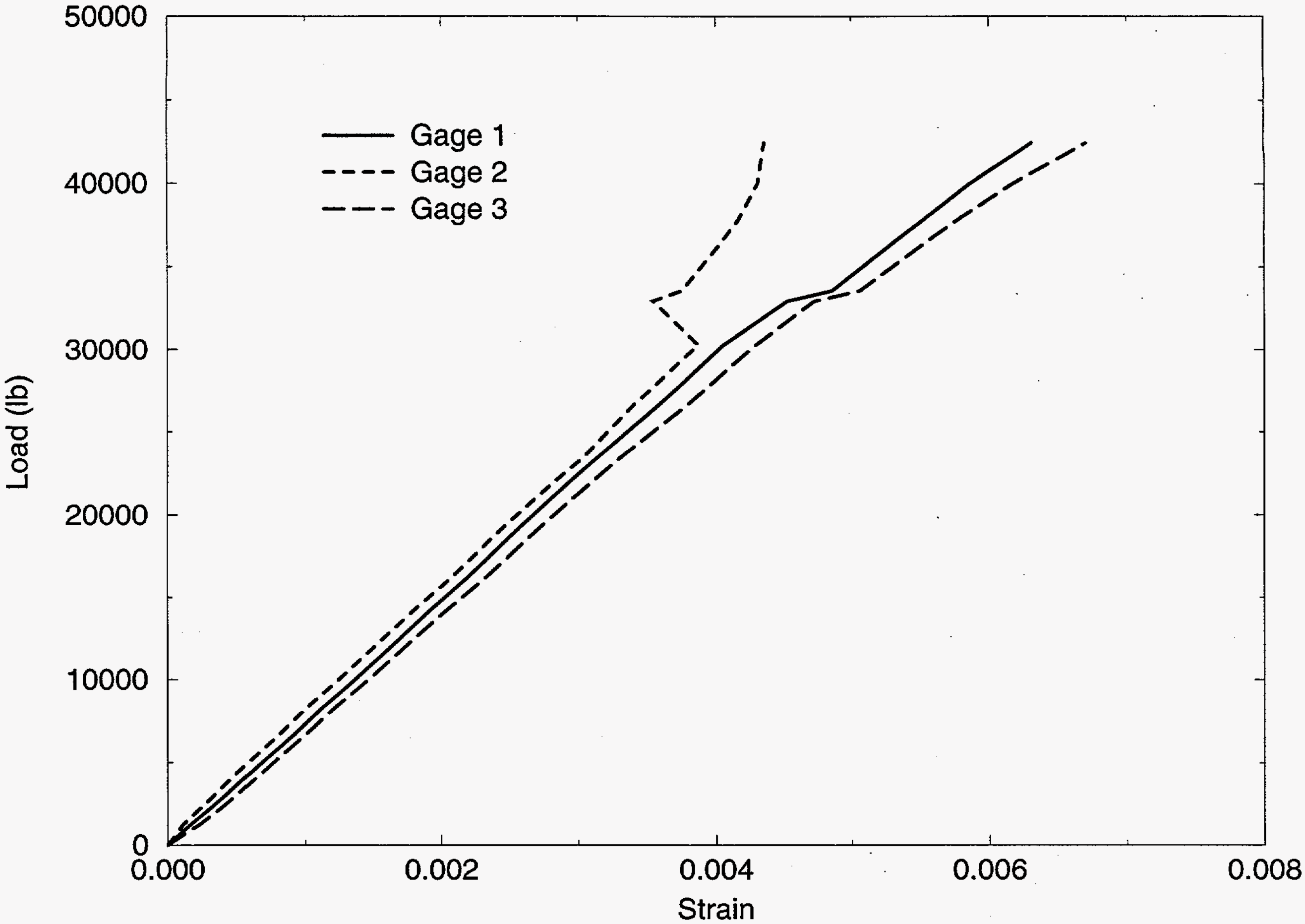

Figure 4. Strain Gage Data - Tapered Adherend Joint

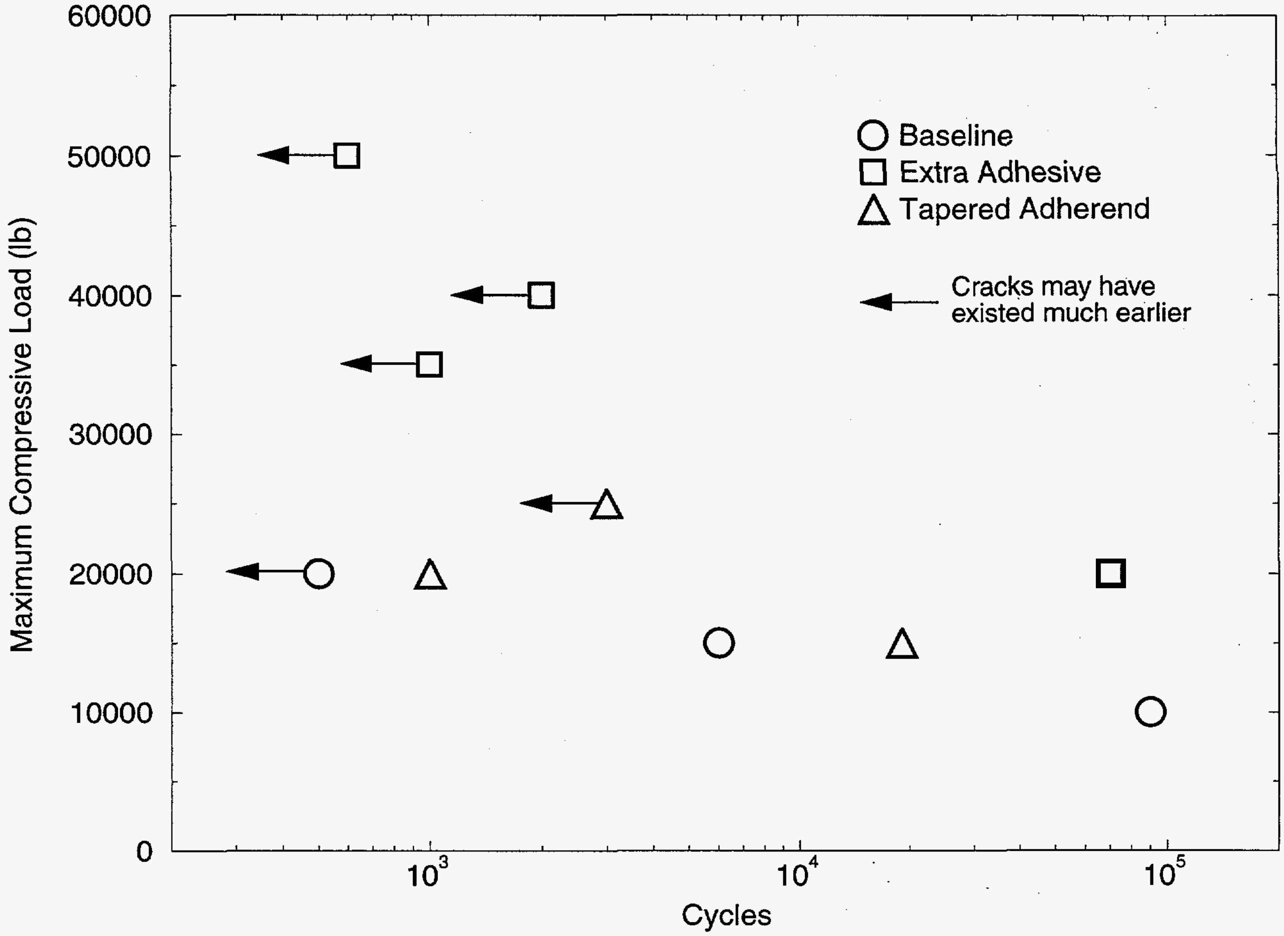

Figure 5. Cyclic Test Results

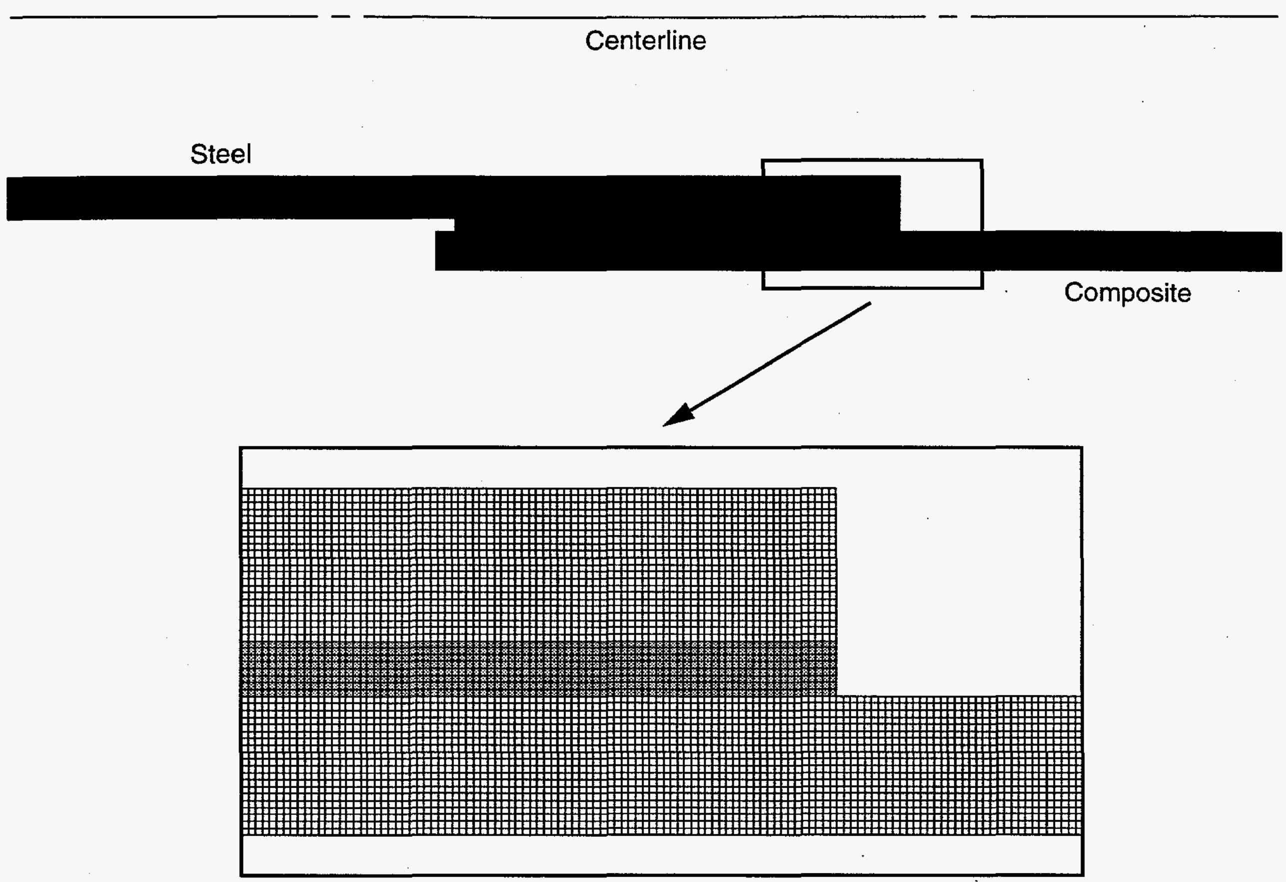

Figure 6. Axisymmetric Finite Element Mesh (Baseline Design)

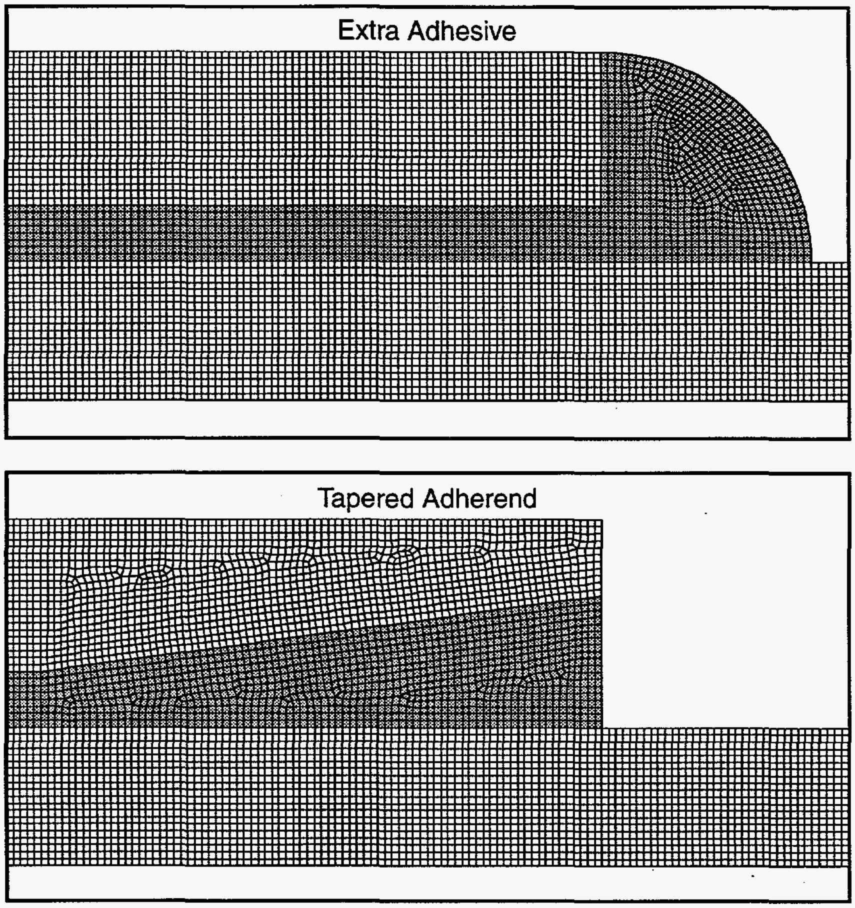

Figure 7. Details of Alternative Finite Element Meshes

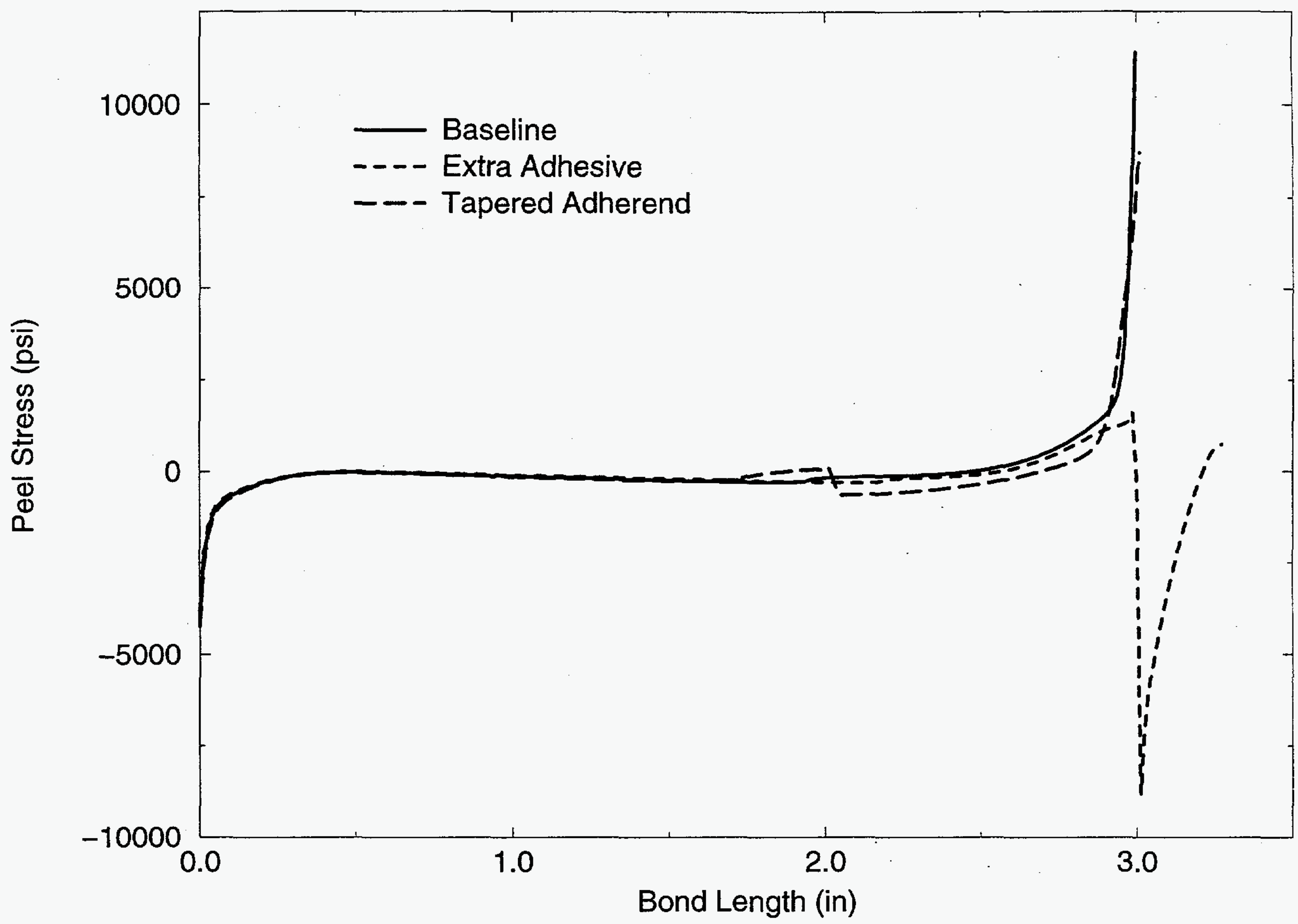

Figure 8. Peel Stresses Due to Compressive Axial Load

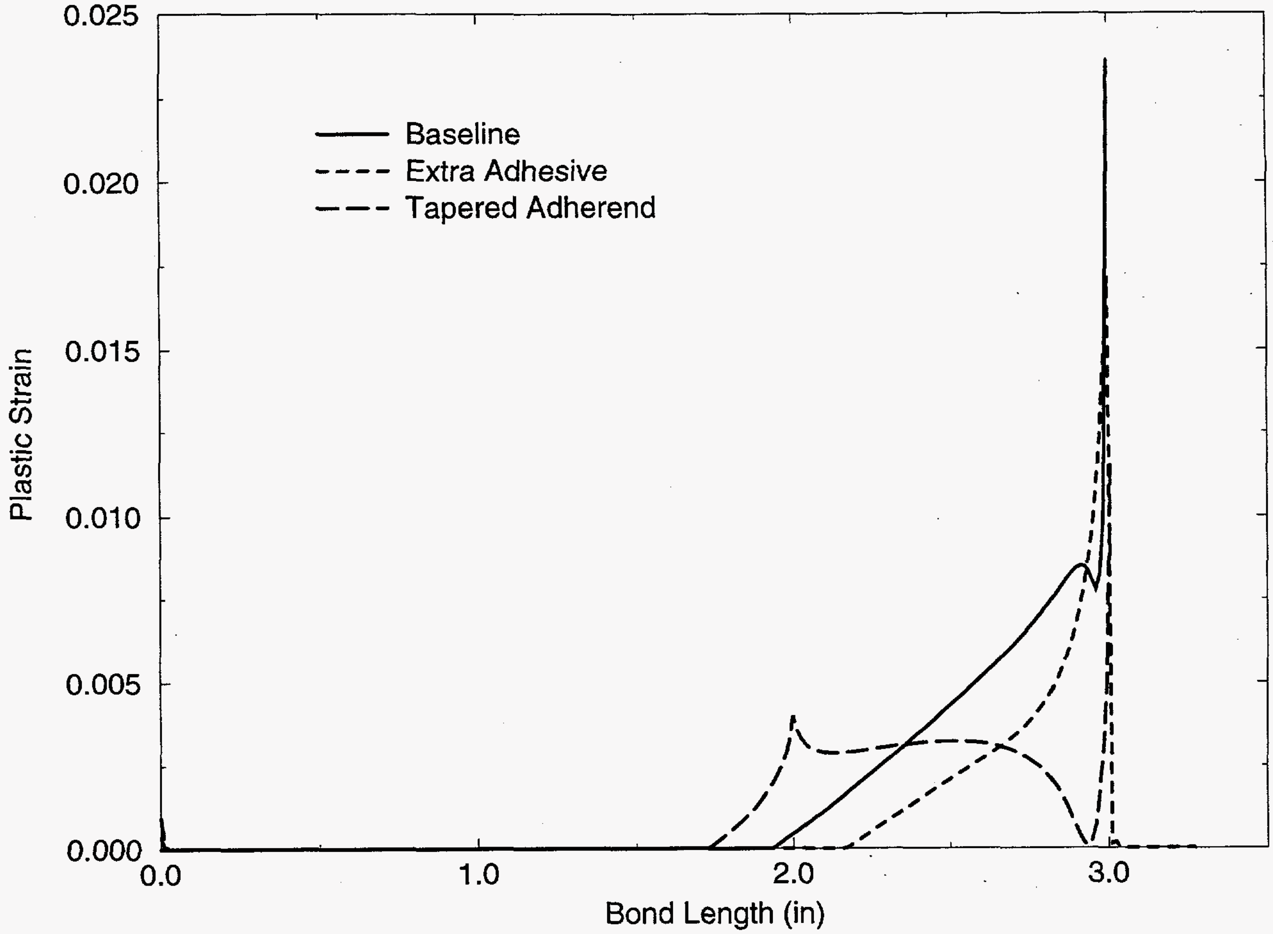

Figure 9. Plastic Strains Due to Compressive Axial Load

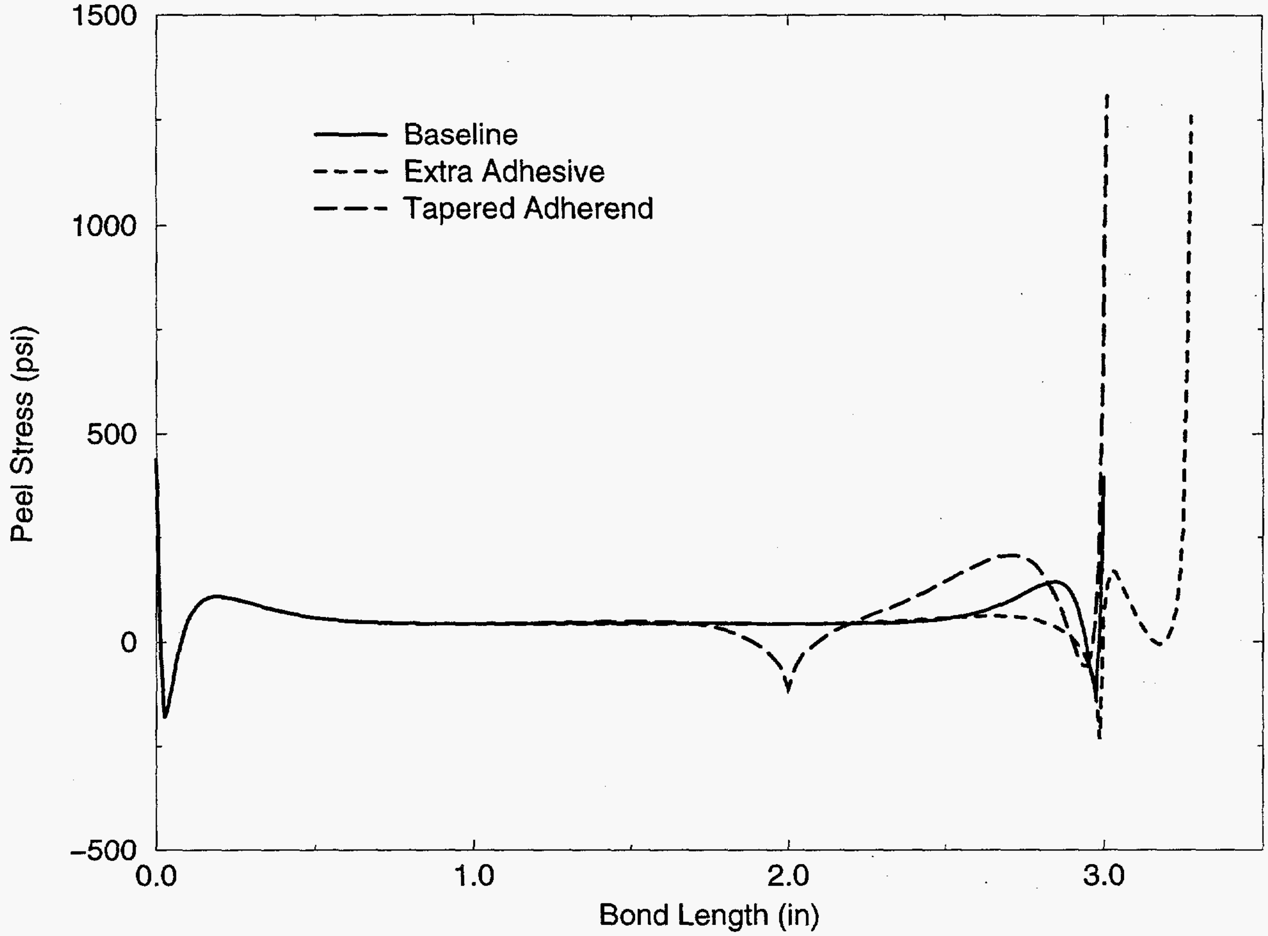

Figure 10. Peel Stresses Due to Adhesive Contraction